GeoMin3D: Pushing the envelope in electrical and EM data interpretation

Guy Marquis, Ali Mohand-Said, Alessandro Vinciguerra, Jean-Francois Girard, University of Strasbourg - ITES
Grant Harrison, Shawn Dempsey, Orano Canada Inc.
Elodie Williard, Orano Mining

gmarquis@unistra.fr, jf.girard@unistra.fr

The GeoMin3D project

GeoMin3D is joint industry-academic program that aims to bring a paradigm shift in unconformity-related uranium deposit exploration by leveraging our scientific and technological findings into innovative exploration technologies. The program aims to improve data acquisition and modeling processes, to bring out new scientific and technical concepts to favor a better understanding of the deposits and their targeting, to improve the use and usability of variable datasets and promote reconciliation between geophysical and geological information. Dr Julien Mercadier from Nancy presents an overview of the GeoMin3D project in a nearby poster presentation. This poster focuses on the geophysical developments of the project.

GeoMin3D partners are Laboratoire GeoRessources, Nancy, Institut Terre et Environnement de Strasbourg and Orano Mining. Funding for the project is provided by Orano and ANR (France's equivalent of NSERC).

Geophysics in the Athabasca

The Athabasca Basin is a world-class uranium mining province hosting high-grade high-tonnage deposits (Figure 1 Left). Uranium mineralization is found at the unconformity (UC) where Proterozoic basin sediments overlie Archean to Paleoproterozoic metamorphic basement rocks. Deposits are also closely associated to steeply-dipping graphite-bearing faults and shear zones. Graphite-rich faults acted as hydrothermal fluids pathways. Fluid circulation led to clay alteration of hosting rock and uranium mineralization (Figure 1 Right).

Thus, the association of graphite-rich faults and alteration haloes correspond to a target for uranium exploration. Electrical resistivity of graphitic conductors is ranging from few $\Omega.m$ to few tens of $\Omega.m$ while basin sediments and basement rocks have resistivities ranging from 1000 $\Omega.m$ to 10000 $\Omega.m$. Alteration of hosting rocks decreases their resistivity (Figure 1D). Thus, geophysical methods sensitive to electrical resistivity are preferred to identify the geological structures associated to uranium mineralization. When looking for uranium deposits in the Athabasca basin, Time-Domain Electromagnetic (TDEM) methods are used to locate graphitic faults, while Direct-Current Resistivity (DC) methods are used to identify alteration haloes (e.g. Nimeck and Koch 2008).

Although TDEM and DC methods are sensitive to electrical resistivity, the signals measured do not carry the same information about the subsurface. TDEM and DC dataset are usually processed separately. Graphitic conductors' location and geometry are in practice well identified using plate-modelling software or an inversion algorithm. Signal from graphitic faults and alteration haloes are recorded in DC resistivity datasets. However, on inversion results, the footprint of graphitic faults overprints the signature from possible contrasts associated to alteration in the host-rocks.

Taking advantage of their specific sensitivity in a 3D joint inversion, we are expecting to constrain the extent of the graphitic conductors, allowing to model the resistivity contrast within sandstones and close to the unconformity, related to fluid flow and recorded in the signal of DC data.

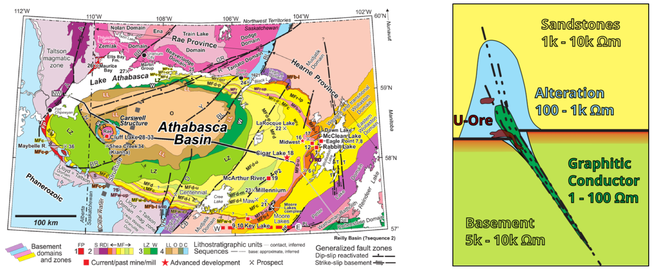

Figure 1: Left: Major structures of Athabasca Basin, Right: Simplified Geological Model of Athabasca U-deposits (Modified from Jefferson et al., 2007).

References

[1] Aquino M., Marquis G., and Vergne J. Joint one-dimensional inversion of magnetotelluric data and surface-wave dispersion curves using correspondence maps. *Geophysical Prospecting*, 2022.

[2] ter Braak C.J.F. and Vrugt J.A. Differential evolution Markov chain with snooker updater and fewer chains. *Statistics and Computing*, 2008.

[3] Cockett R., Kang S., Heagy L.J., Pidlisecky A., and Oldenburg D.W. SimPEG: An open source framework for simulation and gradient based parameter estimation in geophysical applications. *Computer and Geosciences*, 2015.

[4] Conn A.R., Gould N.I.M., and Toint P.L. *Trust Region Methods*. Society of Industrial and Applied Mathematics, 2000.

[5] Evensen G., Raanes P.N., Stordal A.S., and Hove J. Efficient implementation of an iterative ensemble smoother for data assimilation and reservoir history matching. *Frontiers in Applied Math and Stats*, 2019.

[6] Lenders F., Kirches C., and Potschka A. trlib: A vector-free implementation of the GLTR method for iterative solution of the trust region problem. 2016.

[7] Nimeck G. and Koch R. A progressive geophysical exploration strategy at the Shea Creek uranium deposit. *The Leading Edge*, 2008.

[8] Nocedal J. and Wright S.J. *Numerical Optimization*. Springer, 2006.

[9] Raiche A., Sugeng F., and Wilson G. Practical 3D EM inversion – the P223F software suite. *ASEG Extended Abstracts*, 2007.

[10] Yang D., Oldenburg D.W., and Haber E. 3-D inversion of airborne electromagnetic data parallelized and accelerated by local mesh and adaptive soundings. *Geophysical Journal International*, 2013.

3D Inversion of moving-loop TEM and DC data using trust-regions

(PhD thesis of now Dr. Ali Mohand-Said, amohandsaid@unistra.fr)

Joint Inversion methodology

Our joint inversion methodology finds a single resistivity model minimizing the square of the L2-norm of weighted TDEM and DC data discrepancies. Additional weights (w_{em} and w_{dc}) are added to DC and EM data :

$$w_{em} = A_{em}\frac{N_{data}}{N_{em}} \quad w_{dc} = A_{dc}\frac{N_{data}}{N_{dc}}$$

N_{em}, N_{dc} and N_{data}, respectively correspond to the number of EM, DC and total data, and are used to account for the unequal amounts of data between the datasets. A_{em} and A_{dc} are factors tuned to prioritize one or the other dataset. Their sum must be equal to one (Aquino et al. 2022).

Forward modeling of TDEM and DC responses were done using SimPEG codes (Cockett et al. 2015; Heagy et al. 2018), which also allows to compute the fields and their adjoints.

Computing accurate solutions to DC and TDEM forward problems requires different discretizations. As shown in (Yang et al. 2014), computational speed up can be achieved by decomposing TDEM forward problem, in a set of simulations suited to each individual stations and thus using lighter discretizations. We thus define our resistivity model, or inverse model, on a grid adapted to the resolution of our dataset and from this grid, we interpolate this model on a set of simulation grids, suited to DC and profiles and EM stations, using a volume averaging operator, implemented in SimPEG codes. Predicted data and gradients are calculated on these grid before being interpolated back to the inversion grid.

The inverse problem is solved using a Lanczos trust-region algorithm (Conn et al. 2000, Nocedal and Wright 2006, Lenders et al. 2016).

Area of interest and surveys configuration

The area of interest is in the eastern part of the Athabasca basin. A TDEM Moving Loop ground survey was acquired in 2015. Measurements of magnetic flux were made over several lines oriented N-S, perpendicular to previously identified magnetic and conductive trends. For our work we selected vertical component of magnetic field over 15 time gates ranging from 0.1 ms to 2.0 ms at 154 stations, along five profiles, with a spacing of 200m. Receivers were located 800m to the north of the 400m-edge square loop transmitter. Data from a Pole-Dipole survey acquired in 2016 in the same area were available. We selected voltage data from three profiles coincident with the Moving-Loop measurements. The dipole length is 100m, and the current injections were made every 100m. Profiles selected for inversions are highlighted in white (Figure 2).

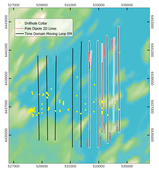

Figure 2: Map of the area of interest. Red dashed lines represents DC resistivity profiles, Black lines to EM profiles. Profiles highlighted in white are those selected for inversion. Yellow dots correspond to drillholes collar positions.

Field data inversion

Figure 3 shows depths slices at 500 m depth of inverse model obtained from the standalone inversions of DC and EM data, and from the joint inversion. EM and joint inversions results are showing conductive anomalies that follow the graphitic conductors intersected by drillholes. Between the easternmost profiles, there is an highly conductive artifact on the EM inversion result, that is clearly mitigated on the joint inversion, due to the fact that there are DC resistivity data to illuminate this area of the subsurface. The conductive anomalies on the joint inversion are also sharper and show greater continuity. It must be noticed that 3D joint inversion allows to visualize a complex network of faults with varying orientation, that may cross-cut each others. Looking at a cross-sections over the three inverse models (Figure 4), along the profile L9500E, we see that the top of the plates are well recovered, on EM and joint inversion models. Subtle variations of resistivity in the range of depth of the sandstones are visible on DC inversion models, these variations are enhanced on the joint inversion model, potentially indicating alteration associated to the southernmost conductors.

These results highlight the benefit in modeling of subsurface conductive structures using joint inversion. It shows a complementarity between DC and EM data allowing to recover sharper strong conductors and enhance the resolution to shallow variation of resistivity. The use of 3D datasets also allow to recover the information on plate orientation.

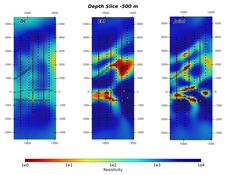

Figure 3: Depth slices at 500 m depth over DC, EM and Joint inversion model. Red dots correspond to electrodes positions, black dots to EM stations positions, and yellow dots to drillhole collars positions. The shaded black lines outline graphitic conductors intersected by drilling.

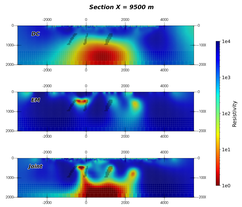

Figure 4: Cross-sections of DC, EM and joint inversion models along profiles L9500.

3D inversion of ERT data through an ensemble-method approach

(Postdoc of Dr. Alessandro Vinciguerra, avinciguerra@unistra.fr)

Inversion algorithm

Bayesian inversion strategy allows to solve the inverse problem taking into account the prior information on the subsurface and assessing the uncertainty in terms of posterior probability density function (pdf). In this work, we present an efficient ensemble-based approach (Evensen et al. 2019) to solve a 3D inverse problem.

Let the model vector $\mathbf{m}$ being the 3D model and $\mathbf{d}$ the observed data, the *pdf* can be expressed as:

$$p(\mathbf{m}|\mathbf{d}) \propto p(\mathbf{m})p(\mathbf{d}|\mathbf{m})$$

where $p(\mathbf{m})$ is the prior distribution associated with the model and $p(\mathbf{d}|\mathbf{m})$ is the likelihood function, which represents the probability of observing the data $\mathbf{d}$ given the considered 3D model $\mathbf{m}$. Since we aim at sampling the *pdf* and not only find its maximum, Evensen et al. (2019) explained that it can be approximated using an iterative and a standard Ensemble Smoother, a method that iteratively updates an ensemble of prior realizations drawn from a prior distribution. The cost function to minimize for each realization *j* is expressed as:

$$T(\mathbf{m}_j) = \frac{1}{2}(\mathbf{m}_j - \mathbf{m}^p)^T\mathbf{C}_m^{-1}(\mathbf{m}_j - \mathbf{m}^p) + \frac{1}{2}(g(\mathbf{m}_j) - \mathbf{d})^T\mathbf{C}_{dd}^{-1}(g(\mathbf{m}_j) - \mathbf{d})$$

where $\mathbf{m}^p$ is the prior mean model, $\mathbf{C}_m$ is the covariance matrix of the model, $\mathbf{C}_{dd}$ is the covariance matrix of the data and g is the forward operator. Each cost function $T(\mathbf{m}_j)$ is minimized through a Gauss-Newton-like method where the sensitivity $\tilde{\mathbf{J}}$ is approximated using the ensemble of models and data, thus avoiding the computationally expensive explicit calculation. The Hessian matrix is the defined as:

$$H(\mathbf{m}_j) = \mathbf{I} + \tilde{\mathbf{J}}^T\mathbf{C}_{dd}^{-1}\tilde{\mathbf{J}}$$

then the iterative Gauss-Newton scheme to minimize the cost functions can be defined as:

$$\mathbf{m}_j^{i+1} = \mathbf{m}_j^i - \gamma(\mathbf{I} + \tilde{\mathbf{J}}^T\mathbf{C}_{dd}^{-1}\tilde{\mathbf{J}})^{-1} \times (\mathbf{m}_i + \tilde{\mathbf{J}}^T\mathbf{C}_{dd}^{-1}(\mathbf{g}(\mathbf{m}_j) - \mathbf{d}))$$

where $\gamma \in (0, 1]$ is introduced as a step-length parameter and $\mathbf{I}$ is the identity matrix. After the minimization of all the cost functions $T(\mathbf{m}_j)$, the ensemble of final models approximate the pdf, from which the uncertainty is computed.

3D ERT synthetic dataset

To test the algorithm, we apply the inversion strategy to a synthetic 3D ERT dataset. The survey is composed by six lines of length 2000 m and dipole-dipole configuration with electrode spacing of 100 meters (Figure 5 Left). The data is simulated using Simpeg open source code (Cockett et al. 2015) an 3D half-space discretized through a Octree-mesh. The total number of 3D cells for the forward modeling is 85026, whereas for the inversion is 71176. The synthetic half-space is composed by a background resistivity of $100\ \Omega \cdot m$ and two spheres of low and high resistivity, $10\ \Omega \cdot m$ and $1000\ \Omega \cdot m$ respectively. The computed data along the horizontal line is represented in Figure 5 Right.

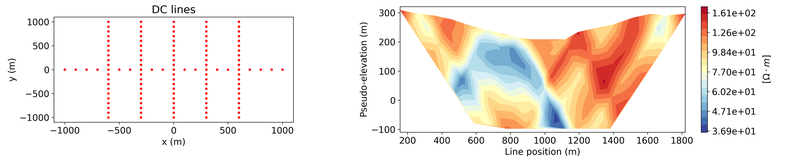

Figure 5: Left: Plane view of DC survey lines, Right: 2D pseudosection associated to one of the survey lines.

The computational time for an ensemble of size 1000 is about 8 hours using a laptop equipped by Intel(R) Core(TM) i5-9400H CPU @ 2.50GHz. The approach allows to represents the result as mean model (Figure 6 Left) and *pdf* (Figure 6 Right) for selected cells of the model.

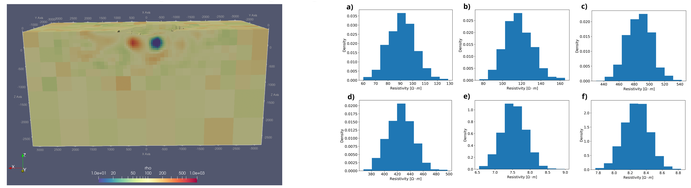

Figure 6: Left, clip of the mean 3D model. Right, posterior *pdf* associated with six cells.